Desalination and Water Treatment
www.deswater.com
doi: 10.5004/dwt.2020.25668

190 (2020) 215–225
June

Granular activated carbon as an adsorbent for simultaneous removal of nitrosodipropylamine (NDPA) and nitrosodibutylamine (NDBA) from water

Chao Zhou[a,b,c], Changxuan He[a], Jinchao Bai[c], Jianhai Sun[d], Hao Wang[d], Yiqiong Yang[b,*], Naiyun Gao[e], Xiaodong Zhang[b,*]

[a]*Shanghai Municipal Planning and Design Institute Co., Ltd., Shanghai 200031, China, emails: zhouchaolzxm@163.com (C. Zhou), hechangxuan@163.com (C.X. He)*
[b]*School of Environment and Architecture, University of Shanghai for Science and Technology, Shanghai 200093, China, Tel. +86 15921267160; emails: yangyiqiong@usst.edu.cn (Y.Q. Yang), fatzhxd@126.com (X.D. Zhang)*
[c]*Shanghai Compulory Verification Center for Watermeters Co., Ltd., Shanghai 201900, China, email: 315633594@qq.com (J.N. Bai)*
[d]*Shanghai Municipal Engineering Design Institute (Group) Co., Ltd., Shanghai 200092, China, emails: 13402045969@126.com (J.H. Sun), stargazewang@126.com (H. Wang)*
[e]*State Key Laboratory of Pollution Control and Resources Reuse, College of Environmental Science and Engineering, Tongji University, Shanghai 200092, China, email: gaonaiyun1@126.com (N.Y. Gao)*

Received 27 July 2019; Accepted 5 February 2020

ABSTRACT

Nitrosodipropylamine (NDPA) and nitrosodibutylamine (NDBA) are two representative nitrosamines that are known as emerging nitrogenous disinfection by-products in water with potent mutagenicity, teratogenicity, and carcinogenicity. In this study, laboratory-scale studies were carried out to concurrently remove both NDPA and NDBA from water. Key factors affecting the removal rate and adsorption capacity were studied. The treatment performance was heavily influenced by granular activated carbon (GAC) types, initial solution pH, reaction temperature, and water matrices, but appeared to be affected by initial concentration slightly. Within 48 h, 0.1 g/L cocoanut GAC (YK), advantageous over nutshell GAC (GK), and coal-based GAC (MZ), adsorbed >90% of 0.20 mg/L NDPA and NDBA at pH = 7 and 298 K. The adsorption kinetics and isotherm patterns could be well-described by pseudo-first-order reaction kinetics model and the Langmuir model. Thermodynamics analysis validated that the adsorption processes for both NDPA and NDBA were spontaneous and endothermic. Results showed that GAC might be an excellent agent to prevent water pollution caused by nitrosamines.

Keywords: Adsorption; Nitrosodipropylamine (NDPA); Nitrosodibutylamine (NDBA); Kinetics; Thermodynamics

1. Introduction

Recently, more and more pollutants have attracted the attention of researchers [1–7]. Nitrosamines (NAms) [8] represent a class of emerging disinfection by-products (DBPs) [9–13] that are formed through reactions between natural organic matters and disinfectants during chlor(am)ination of drinking water. NAms are of a great health concern due to their potent mutagenicity, teratogenicity, and carcinogenicity [14]. Representative NAms include nitrosodimethylamine (NDMA), nitrosomethylethylamine (NMEA), nitrosopyrrolidine (NPYR), nitrosodiethylamine (NDEA), nitrosopiperidine (NPIP), nitrosomorpholine (NMOR), nitrosodipropylamine (NDPA), nitrosodibutylamine (NDBA), and nitrosodiphenylamine (NDPhA) [8]. Recently, various NAms [15–18] have been frequently detected in water and

* Corresponding authors.

1944-3994/1944-3986 © 2020 Desalination Publications. All rights reserved.

wastewater, and a few countries have started to set up their regulation levels in the water. The USA California health ministry has set 10 ng/L as standards for three kinds of typical NAms, including NDMA, NDEA and NDPA [19,20]. The US EPA non-controlling pollutants Detection Rule-2 (UCMR-2) included six NAms (NDMA, NDEA, NDPA, NPYR, NMEA, and NDBA) into a list of test objects in the drinking water system [21]. Moreover, five individual NAms (NDMA, NDEA, NDPA, NPYR, and NDPhA) have entered the EPA's Contaminant Candidate List 3 in 2009 [22]. Among the NAms, NDPA, and NDBA are characterized by relatively high molecular weights and weak polarity. Planas et al. [23] reported 2.4 ng/L NDBA level in a chlorinated reservoir of Spain. Templeton and Chen [18] measured eight NAms in six water distribution systems in the United Kingdom and found that the maximal NDBA concentration was 6.4 ng/L. Wang et al. [15] monitored nine NAms in the raw water and finished water of 12 Chinese waterworks, and found that NDMA, NDEA, NDBA, and NMOR were the most commonly detected. In particular, NDBA ranged at 1.0–19.9 ng/L and 0.4–3.4 ng/L in raw water and finished water, respectively.

Different water treatment technologies have been studied for removal of organic matters from water, such as coagulation, solvent extraction, liquid membrane permeation, adsorption by ion-exchange resin, and activated carbon (AC) [24], and advanced oxidation processes [25–27]. Amongst the treatments, AC-induced adsorption has increasingly gained great attention due to its huge specific surface area, tailored pore distribution, high degree of surface reactivity, little formation of by-products [28,29], low cost, and convenient operation [30,31]. In previous studies, AC was commonly used as adsorbent in water treatment independently [32–35], such as β-ionone [36], brilliant green dye [37], and EDTA (ethylenediaminetetraacetic acid) [38], and adsorption kinetics, isotherm, and thermodynamics tests were conducted. Especially, Dai et al. [39] applied AC as sorbent for NDMA, and found that the adsorption process followed the Freundlich model, and the adsorption capacity was significantly influenced by the micropore size, relative pore volume, and other surface characteristics. Nevertheless, multiple compounds, rather than a single one, typically co-exist in water in a real ambient condition. Therefore, it would be more appropriate to study the simultaneous adsorption of two or more compounds by AC from water. Simultaneous adsorption tests provide valuable information regarding the fractions of sites occupied by different solutes tested, their affinities towards these sites, and the lateral interactions between the solutes in a mixed solution [40–43]. AC adsorption of two representative taste and odor compounds (2-isopropyl-3-methoxy pyrazine and 2-isobutyl-3-methoxy pyrazine) in drinking water was investigated, and the modified Freundlich equation best fit the experimental data during the adsorption isotherm tests, and the pseudo-first-order kinetics well-described the adsorption kinetics pattern [44].

Recently, some adsorbents are used for the removal of NAms [45–48]. But, little literature is known on AC adsorption for a mixed NAms solution. The objective of this study is to explore simultaneous adsorption of traceable NDPA and NDBA (two representative NAms) in water. Adsorption kinetics, isotherm, and thermodynamics tests are conducted to determine the AC adsorption capacities for the both NAms, and evaluate the effects of AC types, pH, initial NAms concentrations, and water matrices on the treatment efficiency.

2. Materials and methods

2.1. Chemicals

All chemicals were at least analytical grade, except noted. Solutions were prepared using ultrapure water (18.2 MΩ cm) produced from a Milli-Q Water Purification system (Billerica, Massachusetts, USA). Standard solutions of NDPA (5 g/L) and NDBA (2 g/L) were purchased from Sigma-Aldrich (Oakville, ON, Canada). Basic physical and chemical characteristics of both NAms are shown in Table S1 [8,17,18]. The mixing stock solutions of NDPA and NDBA (2 mg/L) were prepared in methanol (HPLC grade) (Sigma-Aldrich, Oakville, ON, Canada). Formic acid, NaOH, HCl, KH_2PO_4, and Na_2HPO_4 (AR grade) were purchased from Sinopharm Chemical Reagent Co. Ltd., China used without further purification. Phosphate buffer (pH = 7.0) was prepared by dissolving 62 g KH_2PO_4 and 78 g Na_2HPO_4 into 1 L ultrapure water [49]. All the glassware used in the experiments were soaked in an H_2SO_4–$K_2Cr_2O_7$ solution overnight, and then rinsed by tap water and distilled water three times, respectively.

2.2. Characteristics of granular activated carbon

Three commercial granular activated carbon (GAC) types, including cocoanut activated carbon (YK) (Calgon Carbon Corporation, China), nutshell activated carbon (GK) (Calgon Carbon Corporation, China), and coal-based activated carbon (MZ) (Activated Carbon Huaqing Group Co., Ltd., Shanxi, China), were used in this study. Their basic physical and chemical properties are shown in Table S2. Particularly, the structural characteristics of YK are shown in Table S3 [50], including the specific surface area, pore volume and pore size of GAC that were measured with the nitrogen adsorption isotherm using the Brunauer–Emmett–Teller (BET) method (ASAP 2010 Micromeritics instrument), United States. Prior to all experiments, the AC materials were rinsed repeatedly with tap water and then ultrapure water to remove any fine particle and soluble materials, then dried in an oven at 105°C for 24 h, and finally stored in a desiccator.

2.3. Chemical analysis

NDPA and NDBA were measured using liquid chromatograph (LC)-mass spectrometer (MS)/MS (Waters, Thermo Scientific* TSQ Quantum Access MAX, USA). Calibration solutions (1–500 μg/L) were prepared using a mixed solution of 2 mg/L NDPA and NDBA. LC (Waters) was coupled directly to a triple stage quadrupole MS (Thermo Scientific* TSQ Quantum Access MAX, USA) with ion sources. LC Quan software was used for data acquisition and analysis. A C_{18} capillary column (100 mm × 2.1 mm i.d., 5 μm) (Thermo Scientific) was used for separation at 30°C. The mobile phase was composed of solvent A (0.1% formic acid in water (Optima grade)) and solvent B (100% methanol) [51]. The fraction of the solvent B was increased

from 60% to 90% over 6 min, and then returned to 60% over 0.10 min, followed by a 2 min re-equilibration prior to the next sample injection. The flow rate was 0.15 mL/min, and the sample injection volume was 10 μL. Positive electrospray ionization combined with the selected-reaction monitoring (SRM) mode was used. The optimization of MS conditions was performed by infusing a mixture of NDPA and NDBA (1 mg/L each in ultrapure water) using a syringe pump. The optimal ionspray parameters were as follows: spray voltage at 3,500 V, vaporizer temperature at 300°C, sheath gas pressure at 40 arb, aux gas pressure at 10 arb, and capillary temperature at 270°C. The product ions, tube lens offset, and collision energies (CE) were optimized for the individual analytes, as shown in Table S4. Dissolved organic carbon (DOC) was quantified using a TOC analyzer (TOC-VCPH, SHIMADZU, Japan). Zeta analyzer (zetasizer nano zs90, UK) was used to determine zeta potential of the GAC surface. Solution pH was measured using a pH meter (PHS-3G, Leici Corp., China).

2.4. Adsorption procedure

All tests were carried out in 250 mL stoppered glass vials containing 200 mL NDPA and NDBA mixed solution (C_0 = 0.05–0.50 mg/L). The vials were installed in a temperature-controlled orbital shaker (HYG-A, China) at a constant rotation speed of 160 rpm, which could maintain a desirable reaction temperature and provide a complete solution mixing state. If needed, initial solution pH was adjusted to a desirable value (3–11) with 0.1 M HCl and 0.1 M NaOH solutions. The adsorption was initiated once appropriate amounts of GAC were added. In a typical kinetics test, 1 mL sample was collected with syringes at each designated sampling time. In typical adsorption isotherm tests, the adsorption reaction would proceed for 48 h prior to sample collection. Thermodynamics tests were conducted at the identical conditions with adsorption isotherm tests, except that reaction temperatures were controlled at 288, 298, 308, and 318 K, respectively. Once collected, the sample was filtered through 0.70 μm fiberglass membrane for further analysis. At a minimum, all experiments were performed in triplicate. Symbols and error bars in figures represent the average values and standard deviations of the data, respectively.

2.5. Data process

The amount of organics adsorbed per unit adsorbent mass is calculated as follows [50]:

$$q = \frac{\left(C_0 - C_t\right)V}{m} \tag{1}$$

$$q_e = \frac{\left(C_0 - C_e\right)V}{m} \tag{2}$$

where q and q_e are the amounts adsorbed to GAC at time 0 and at chemical equilibrium, respectively (mg/g); C_0 and C_t are the concentrations of NAms in bulk solution at time 0 and any specific time t (mg/L), respectively; V is the solution volume (L); m is the mass of GAC (g); C_e is the equilibrium concentration of NAms in bulk solution (mg/L).

The experimental data are fitted with different kinetic models (pseudo-first-order, pseudo-second-order, and pseudo-third-order) and equilibrium models (Langmuir, Freundlich, Temkin, and Dubinin–Radushkevich). The models are evaluated by the coefficient of determination (R^2).

The three kinetics Eqs. (3)–(5) are listed as below [52,53]:

Pseudo-first-order kinetics:

$$q_t = q_e\left(1 - \exp\left(-k_1 t\right)\right) \tag{3}$$

Pseudo second-order kinetics:

$$q_t = \frac{q_e^2 k_2 t}{1 + q_e k_2 t} \tag{4}$$

Pseudo third-order kinetics:

$$q_t = q_e\left(1 - \frac{1}{\sqrt{k_3 t q_e^2 + 1}}\right) \tag{5}$$

where q_t and q_e are the amounts of NAms adsorbed to GAC at any time t and chemical equilibrium (mg/g), respectively; and, k_1 (h^{-1}), k_2 (g/(mg h)), and k_3 ($g^2/(mg^2\ h)$) are the rate constants of pseudo-first-, second-, and third-order reactions, respectively.

The data in adsorption isotherm tests are used to fit the Langmuir, Freundlich, Temkin, and Dubinin–Radushkevich equations.

The Langmuir isotherm model is listed as below [54]:

$$q_e = \frac{K_L a_L C_e}{1 + a_L C_e} \tag{6}$$

where K_L is the mono-layer adsorption capacity (mg/g); and a_L is the energy of adsorption (L/mg).

The Freundlich isotherm equation is listed as below [54]:

$$q_e = K_f C_e^{\frac{1}{n}} \tag{7}$$

where K_f is the adsorption capacity ((mg/g)·$(L/g)^{1/n}$); and n is the adsorption intensity.

The Temkin isotherm model is expressed as below [54]:

$$q_e = \frac{RT}{b}\ln\left(K_{\mathrm{Te}} C_e\right) \tag{8}$$

where b is related to adsorption energy (kJ/mol); K_{Te} is the Temkin isotherm constant (L/g); R is the gas constant (8.314×10^{-3} kJ/K mol); and T is the absolute temperature (K).

The Dubinin–Radushkevich isotherm model is listed as follows [54]:

$$q_e = q_m \exp\left(\frac{\left(RT\ln\left(1 + \frac{1}{C_e}\right)\right)^2}{-2E^2}\right) \tag{9}$$

where q_m is the saturation adsorption capacity (mg/g) and E is the energy of adsorption (kJ/mol).

Gibbs free-energy change ($\Delta G°$) of the adsorption process can be determined by the classical Van't Hoff equation [55].

$$\Delta G° = -RT \ln K_{ad} \tag{10}$$

where $\Delta G°$ is the free-energy change (kJ/mol); and K_{ad} is the adsorption equilibrium constant determined above. $\Delta G°$ can also be expressed as below [55]:

$$\Delta G° = -\Delta H° - T\Delta S° \tag{11}$$

where $\Delta S°$ is the change in entropy (kJ/(mol K)); and $\Delta H°$ is the heat of adsorption at a constant temperature (kJ/mol). From the Eqs. (10) and (11), we can conclude:

$$\ln K = \frac{-\Delta G°}{RT} = \frac{\Delta S°}{R} - \frac{\Delta H°}{RT} \tag{12}$$

In Eq. (12), $\Delta H°$ can be determined from the slope of the linear Van't Hoff plot (i.e., the plot of $\ln K_{ad}$ vs. $(1/T)$), using Eq. (13) [55]:

$$\Delta H° = \left[R \frac{d \ln K_{ad}}{d\left(\frac{1}{T}\right)} \right] \tag{13}$$

The $\Delta H°$ corresponds to the isosteric heat of adsorption ($\Delta H_{st,0}$) with zero surface coverage (i.e., $q_e = 0$) [56]. K_{ad} at $q_e = 0$ is obtained from the intercept of the plot of $\ln(q_e/c_e)$ vs. q_e at different temperatures.

3. Results and discussion

3.1. Adsorption kinetics

3.1.1. Effect of GAC types

Effect of the three types of GAC for adsorption of a mixed solution of NDPA and NDBA is shown in Fig. 1. For either of the NAms, the adsorption by any GAC type somewhat followed a similar three-phase kinetics pattern. Within the first 12 h, the adsorption rapidly proceeded, and the amounts of adsorbed pollutants eventually accounted for 50% of the GACs' respective adsorption capacities. In the following 36 h, the adsorption process slowed down. Thereafter, the adsorption almost reached equilibrium. Among the three types of GAC, YK achieved the highest adsorption capacities (1.74 mg NDPA/g and 1.89 mg NDBA/g), followed by GK (1.58 mg NDPA/g and 1.83 mg NDBA/g), and MZ (1.56 mg NDPA/g and 1.82 mg NDBA/g). For any particular GAC, NDBA was slightly more readily adsorbed than NDPA, because NDBA was more hydrophobic due to its greater molecular weight (MW) and octanol-water partition coefficient (NDBA: MW = 144 g/mol, $\log K_{ow}$ = 2.63; NDPA: MW = 130 g/mol, $\log K_{ow}$ = 1.36).

Rate constants, calculated and experimental equilibrium adsorption capacities ($q_{e,cal}$ and $q_{e,exp}$) and regression

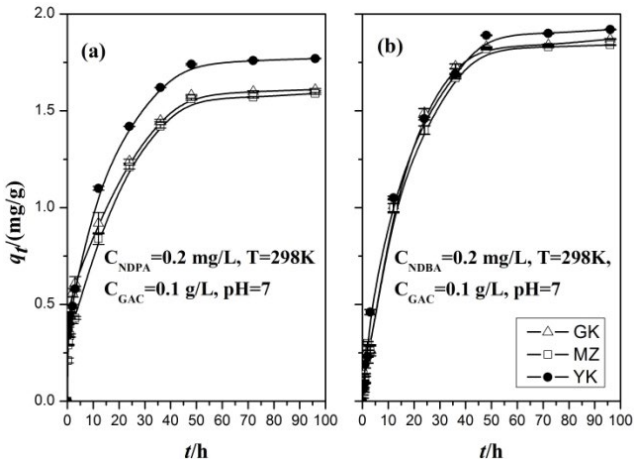

Fig. 1. Effect of GAC types on adsorption kinetics for a mixed solution of NDPA and NDBA (initial NDPA and NDBA concentrations = 0.20 mg/L, C_{GAC} = 0.1 g/L, T = 298 K, pH = 7) (a) NDPA and (b) NDBA.

coefficients R^2 during different GAC adsorption of NDPA and NDBA are summarized in Table 1. Pseudo-first-, second-, and third-order kinetics models were acceptable to describe the kinetics patterns of GAC adsorption of NDPA and NDBA in water (R^2 > 0.90). Among them, the pseudo-first-order kinetics equation appeared to be the best one because it had the lowest relative difference of q_e (Δq_e%), which is defined as below:

$$\Delta q_e\% = \frac{\left| q_{e,cal} - q_{e,exp} \right|}{q_{e,exp}} \times 100\% \tag{14}$$

Physical characteristics of GAC, especially the pore size distribution, are key factors affecting the adsorption performance of GAC for pollutants [57]. The International Institute of Pure and Applied Chemistry (IUPAC) categorized pores of GAC into four types: macropores (>50 nm), mesopores (2–50 nm), the second micropores (0.8–2 nm), and the first micropores (<2 nm) [58]. GAC with abundant pores similar to the size of target molecules has a high adsorption potential for target pollutants. Both NDPA and NDBA are hydrophobic and have very small molecular sizes, and YK has the largest total volumes of micropores. Therefore, YK was the best GAC for adsorption of NDPA and NDBA, so YK was used in the following test.

3.1.2. Effect of initial NAms concentration

The effect of different initial NDPA and NDBA concentrations (mass concentrations of NDPA to NDBA = 1:1) on the adsorption rates of GAC is shown in Fig. 2. $q_{e,cal}$, $q_{e,exp}$, and R^2 during different initial NAms concentrations of NDPA and NDBA are summarized in Table 2. As Table 2 shown, the initial NAms concentration was a key factor to affect the GAC adsorption rate and capacity. At a low concentration (0.05–0.10 mg/L), the GAC adsorption of NDPA and NDBA reached chemical equilibrium within 24 h and the adsorption

Table 1
Effect of GAC types on adsorption kinetics parameters for a mixed solution of NDPA and NDBA

NDPA	First-order kinetics					Second-order kinetics				Third-order kinetics			
	$q_{e,\exp}$ (mg/g)	$q_{e,\mathrm{cal}}$ (mg/g)	k_1 (h^{-1})	R^2	Δq_e (%)	q_e (mg/g)	k_2 (g/(mg h))	R^2	Δq_e (%)	q_e (mg/g)	k_3 ($g^2/(mg^2\ h)$)	R^2	Δq_e (%)
YK	1.74	1.73	0.09	0.9323	0.6	1.82	0.14	0.9635	4.6	2.01	0.19	0.9762	15.5
GK	1.58	1.57	0.29	0.9186	0.8	1.66	0.19	0.9602	5.1	1.83	0.25	0.9704	16.0
MZ	1.56	1.55	0.15	0.9557	0.6	1.68	0.12	0.9666	7.4	1.90	0.13	0.9699	21.5
NDBA													
YK	1.89	1.93	0.07	0.9892	2.2	2.11	0.06	0.9648	11.9	2.38	0.06	0.9480	26.0
GK	1.83	1.87	0.08	0.9976	2.4	2.02	0.10	0.9751	10.3	2.25	0.11	0.9517	23.2
MZ	1.82	1.84	0.08	0.9955	0.9	1.98	0.08	0.9946	8.7	2.26	0.07	0.9944	24.0

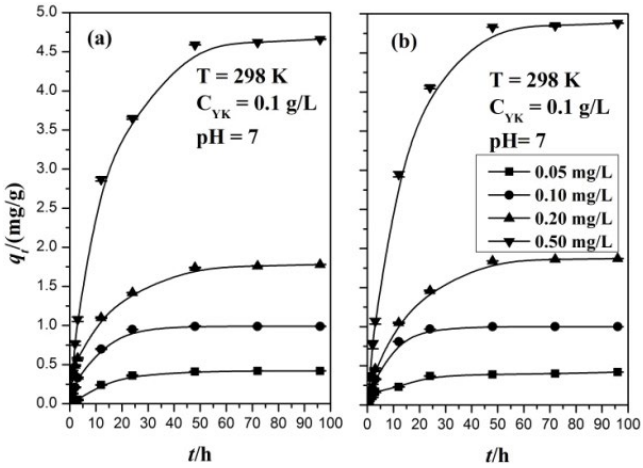

Fig. 2. Effect of initial NAms concentration on GAC adsorption of a mixed solution of NDPA and NDBA (initial concentrations = 0.05, 0.10, 0.20, 0.50 mg/L, C_{YK} = 0.1 g/L, T = 298 K, pH = 7) (a) NDPA and (b) NDBA.

capacities were 0.41 mg NDPA /g and 0.39 mg/g NDBA at the initial concentration of 0.05 mg/L, and 0.99 mg/g NDPA and 1.00 mg NDBA/g at the initial concentration of 0.10 mg/L, respectively. However, when the initial concentrations went up to 0.20 and 0.50 mg/L, the adsorption rate reduced significantly, and the adsorption was completed within 48 h. Meanwhile, the adsorption capacities were 1.74 mg NDPA/g and 1.84 mg NDBA/g at the initial concentration of 0.20 mg/L, and 4.59 mg NDPA/g and 4.83 mg NDBA/g at the initial concentration of 0.50 mg/L, respectively. When the initial concentration of target compounds increased, the fractions of the target compound molecules dropped accordingly, because the amounts of active adsorption sites were almost constant. Therefore, the reaction rate and adsorption capacity of GAC was greatly influenced by the initial concentration of target pollutants.

3.1.3. Effect of the initial pH

Effect of initial pH on the GAC adsorption of NDPA and NDBA is illustrated in Fig. 3, and the solution pH values and GAC zeta potentials before and after adsorption are shown in Table 3. The GAC adsorption capacities for the two NAms followed an order of pH 5.35 > 10.92 > 9.11 ≈ 3.23 > 6.82. Except at pH 3.23, the zeta potentials did not fluctuate greatly during the adsorption process. As shown in Table 3, the effect of initial solution pH was not significant in the removal rate. The GAC adsorption capacity increases slightly from 1.35 mg/g at pH = 6.82 to 1.72 mg/g at pH = 5.35 for NDPA, and from 1.44 mg/g at pH = 6.82 to 1.83 mg/g at pH = 5.35 for NDBA, respectively. It seemed that the surface charge was not a primary factor affecting the adsorption process.

$q_{e,\mathrm{cal}}$, $q_{e,\exp}$, and R^2 of initial pH during GAC adsorption of NDPA and NDBA at different initial pH are summarized in Table 4. At any specific pH, three models were all acceptable to describe the patterns of adsorption kinetics (R^2 > 0.90). With the lowest Δq_e%, the pseudo-first-order kinetics equation appeared to be the best one.

3.1.4. Effect of water matrices

Effect of different water matrices, including ultrapure water, tap water collected from the environmental laboratory at Tongji University (China), and raw water collected from Yangtze River (China), the GAC adsorption capacity for NDPA and NDBA is shown in Fig. 4. The basic physical and chemical characteristics of the tap and raw water samples are shown in Table S5. The removal efficiencies of both NDPA and NDBA in the ultrapure water were >90% within 48 h, significantly greater than those in the raw water and tap water. Compared with ultrapure water, the tap water and raw water had high DOC and UV_{254} relatively, which suggesting that organic compounds in the matrices restricted the GAC adsorption in some degree. Of interest, at identical experimental conditions, the NDBA adsorption capacity was slightly higher than that of NDPA.

3.2. Adsorption isotherms

Experimental and modeled isotherm data of GAC adsorption for NDPA and NDBA at different temperatures (288, 298, 308, and 318 K) are shown in Figs. S1–S4, and the corresponding adsorption isotherm parameters are summarized in Table 5. Among the four tested models, Temkin isotherm was the poorest in terms of R^2 (R^2 = 0.8311 ± 0.0605

Table 2
Effect of initial NAms concentration on adsorption kinetics parameters for a mixed solution of NDPA and NDBA

NDPA	First-order kinetics					Second-order kinetics				Third-order kinetics			
	$q_{e,\exp}$ (mg/g)	$q_{e,\text{cal}}$ (mg/g)	k_1 (h^{-1})	R^2	Δq_e (%)	q_e (mg/g)	k_2 (g/(mg h))	R^2	Δq_e (%)	q_e (mg/g)	k_3 ($g^2/(mg^2\ h)$)	R^2	Δq_e (%)
0.05	0.41	0.43	0.07	0.9959	4.65	0.51	0.14	0.9870	19.61	0.62	0.34	0.9819	33.87
0.10	0.99	0.99	0.12	0.9959	0	1.11	0.13	0.9926	10.81	1.30	0.17	0.9872	23.85
0.20	1.74	1.68	0.13	0.9015	3.57	1.84	0.10	0.9373	5.43	2.10	0.09	0.9482	17.14
0.50	4.59	4.63	0.08	0.9974	0.86	5.37	0.02	0.9975	14.53	6.45	0.01	0.9949	28.84
NDBA													
0.05	0.39	0.39	0.12	0.9430	0	0.43	0.42	0.9690	9.30	0.50	1.54	0.9751	22.00
0.10	1.00	1.00	0.14	0.9958	0	1.12	0.15	0.9870	10.71	1.30	0.20	0.9789	23.08
0.20	1.84	1.87	0.07	0.9962	1.60	2.18	0.04	0.9961	15.60	2.63	0.02	0.9940	30.04
0.50	4.83	4.88	0.08	0.9996	1.02	5.68	0.02	0.9961	14.96	6.83	0.01	0.9923	29.28

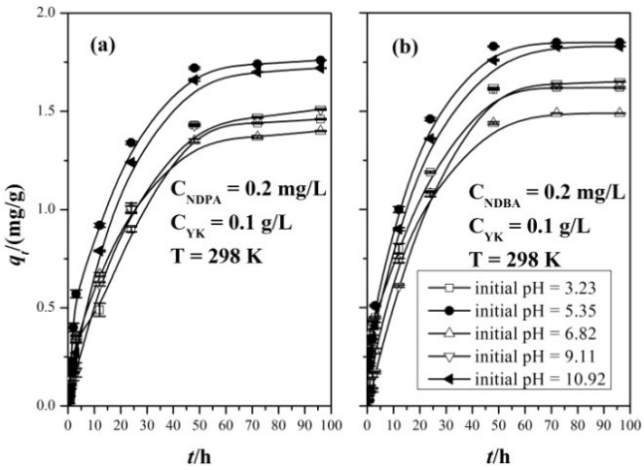

Fig. 3. Effect of the initial pH on GAC adsorption of a mixed solution of NDPA and NDBA (initial concentrations = 0.20 mg/L, C_{YK} = 0.1 g/L, T = 298 K, initial pH = 3.23, 5.35, 6.82, 9.11, and 10.92) (a) NDPA and (b) NDBA.

for adsorption of NDPA and R^2 = 0.7909 ± 0.0431 for adsorption of NDBA). For the NDPA adsorption, Langmuir (R^2 = 0.9797 ± 0.0056) and Dubinin–Radushkevich isotherms (R^2 = 0.9842 ± 0.0046) better fit the measured data than the Freundlich model (R^2 = 0.9602 ± 0.0189). And for NDBA adsorption, Langmuir (R^2 = 0.9796 ± 0.0081) and Freundlich isotherms (R^2 = 0.9867 ± 0.0049) were more appropriate to describe the isotherm data than the Dubinin–Radushkevich equation (R^2 = 0.9706 ± 0.0197). Therefore, the Langmuir model was an appropriate isotherm equation for GAC adsorption of both NAms molecules at 288–318 K.

Table 3
pH and zeta potentials on GAC adsorption of NDPA and NDBA

Initial pH	Final pH	Initial zeta potential (mV)	Final zeta potential (mV)
3.23	2.86	0.7	10.7
5.35	5.80	–22.7	–23.6
6.82	6.34	–34.6	–34.9
9.11	8.74	–39.0	–38.5
10.92	9.62	–53.9	–45.0

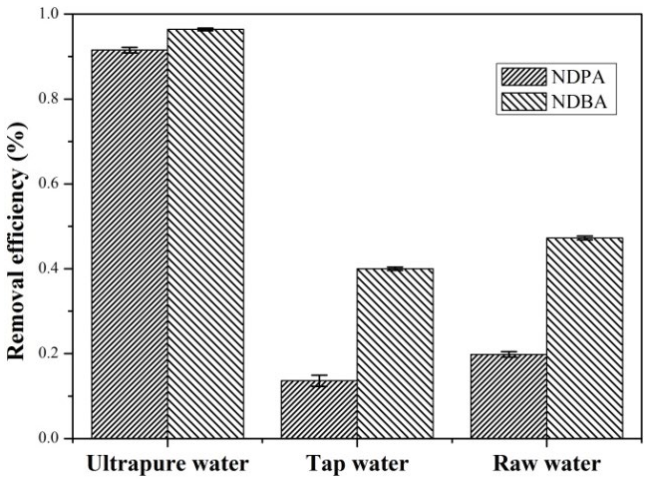

Fig. 4. Effect of water matrices on GAC adsorbing a mixed solution of NDPA and NDBA (initial concentrations = 0.20 mg/L, C_{YK} = 0.1 g/L, T = 298 K, t = 48 h).

3.3. Adsorption thermodynamics

Thermodynamic parameters during the adsorption processes are summarized in Table 6. For the GAC adsorption of NDPA or NDBA, $\Delta H°$ and $\Delta S°$ were positive, while $\Delta G°$ was negative. Of note, the $\Delta H°$ values were below 20 kJ/mol, which suggests that the removal was endothermic physical adsorption [59]. With the increasing temperature, the adsorption capacity of YK type increased, as shown in Figs. S1–S4. On the other side, a positive $\Delta S°$ theoretically confirmed that the adsorption was non-reversible, practically demonstrating that both NDPA and NDBA tended to

Table 4
Effect of the initial pH on adsorption kinetics parameters for a mixed solution of NDPA and NDBA

NDPA	First-order kinetics					Second-order kinetics				Third-order kinetics			
	$q_{e,\exp}$ (mg/g)	$q_{e,\mathrm{cal}}$ (mg/g)	k_1 (h^{-1})	R^2	Δq_e (%)	q_e (mg/g)	k_2 (g/(mg h))	R^2	Δq_e (%)	q_e (mg/g)	k_3 ($g^2/(mg^2\ h)$)	R^2	Δq_e (%)
3.23	1.43	1.52	0.04	0.9753	5.92	1.90	0.02	0.9729	24.74	2.35	0.01	0.9736	39.15
5.35	1.72	1.75	0.05	0.9972	1.71	2.13	0.03	0.9943	19.25	2.62	0.01	0.9924	34.35
6.82	1.35	1.73	0.08	0.9790	21.97	1.97	0.05	0.9891	31.47	2.33	0.04	0.9909	42.06
9.11	1.43	1.55	0.04	0.9970	7.74	1.95	0.02	0.9935	26.67	2.44	0.01	0.9917	41.39
10.92	1.66	1.75	0.05	0.9972	5.14	2.13	0.03	0.9943	22.07	2.62	0.01	0.9924	36.64
NDBA													
3.23	1.61	1.60	0.07	0.9151	0.63	1.77	0.06	0.9370	9.04	2.04	0.06	0.9460	21.08
5.35	1.83	1.82	0.06	0.9670	0.55	2.11	0.04	0.9741	13.27	2.51	0.03	0.9760	27.09
6.82	1.44	1.85	0.07	0.9919	22.16	2.13	0.04	0.9950	32.39	2.55	0.03	0.9943	43.53
9.11	1.62	1.75	0.04	0.9946	7.43	2.26	0.02	0.9880	28.32	2.87	0.01	0.9854	43.55
10.92	1.76	1.82	0.06	0.9670	3.30	2.11	0.04	0.9741	16.59	2.51	0.03	0.9760	29.88

Table 5
Adsorption isotherm parameters of GAC adsorption of NDPA and NDBA at different temperatures

NDPA	Langmuir			Freundlich			Temkin			Dubinin–Radushkevich		
	K_L	a_L	R^2	K_f	n	R^2	K_{Te}	b	R^2	q_m	E	R^2
288	4.22	5.18	0.9769	7.79	1.29	0.9720	150.14	4.95	0.8875	3.18	4.67	0.9776
298	4.64	9.83	0.9762	10.46	1.05	0.9743	124.62	5.66	0.7034	4.09	3.99	0.9863
308	5.26	14.00	0.9940	16.26	1.45	0.9829	395.35	3.63	0.9407	5.43	5.75	0.9945
318	7.05	24.15	0.9718	50.87	1.24	0.9117	1,090.06	4.65	0.7928	9.37	6.24	0.9784
NDBA												
288	8.87	2.21	0.9634	10.45	1.20	0.9791	385.95	7.94	0.7730	3.36	4.65	0.9208
298	7.39	9.31	0.9814	25.83	0.89	0.9890	237.36	5.06	0.7462	6.50	3.93	0.9830
308	7.92	15.00	0.9762	43.04	1.21	0.9811	602.33	4.96	0.7434	8.01	5.89	0.9802
318	7.80	35.66	0.9972	49.53	1.38	0.9976	1,321.20	2.71	0.9010	10.39	6.76	0.9982

Table 6
Thermodynamic parameters of NDPA and NDBA adsorption by GAC under different temperatures

NDPA	T (K)	$\ln K_{\mathrm{ad}}$	$-\Delta G°$ (kJ/mol)	$\Delta H°$ (kJ/mol)	$\Delta S°$ (kJ/(mol K))
YK	288	1.095	2.621	15.689	0.0634
	298	1.264	3.132		
	308	1.523	3.899		
	318	1.696	4.484		
NDBA					
YK	288	1.159	2.775	14.592	0.0602
	298	1.341	3.323		
	308	1.543	3.952		
	318	1.731	4.577		

be adsorbed to GAC. The GAC adsorption entropy values of NDPA and NDBA was a process of continual decline because chaotic NDPA and NDBA molecules in water preferentially moved into the relatively regular arrangement on the GAC surface. However, accompanied by the adsorption of NDPA and NDBA molecules, water molecules attached on the GAC surface originally were desorbed back into bulk solution, thus lowering the entropy. The reduction in entropy due to water desorption appeared to be greater than the increase of entropy due to NAms adsorption. Therefore,

$\Delta S°$ was positive. Additionally, a negative $\Delta G°$ indicated that the adsorption processes were spontaneous. It would be noted that the absolute values of $\Delta G°$, $\Delta H°$, and $\Delta S°$ for GAC adsorption of NDPA were greater than those of NDBA adsorption, which demonstrating that NDBA was more readily adsorbed by GAC than NDPA.

4. Conclusions

This study explored GAC as an adsorbent for the simultaneous removal of two representative NAms (NDPA and NDBA) from water. Results showed that the removal rate and adsorption capacity were influenced by a few factors to different degrees, such as GAC types, initial pH, initial NAms concentration, and water matrices. The adsorption could be appropriately explained by pseudo-first-order reaction kinetics model and the Langmuir model. Thermodynamics analysis confirmed that GAC adsorption for both NAms were spontaneous. These findings demonstrate that GAC is a potential alternative to address water pollution caused by NAms and other emerging contaminants.

Acknowledgments

This work was financially supported by the National Natural Science Foundation of China (No. 51508327, 51778565, 51578487).

References

[1] C. Zhang, H. Huang, G. Li, L. Wang, L. Song, X. Li, Zeolitic acidity as a promoter for the catalytic oxidation of toluene over MnO_x/HZSM-5 catalysts, Catal. Today, 327 (2019) 374–381.
[2] Z. Wang, Q. Sun, D. Wang, Z. Hong, Z. Qu, X. Li, Hollow ZSM-5 zeolite encapsulated Ag nanoparticles for SO_2-resistant selective catalytic oxidation of ammonia to nitrogen, Sep. Purif. Technol., 209 (2019) 1016–1026.
[3] L. Wang, G. Yin, Y. Yang, X. Zhang, Enhanced CO oxidation and toluene oxidation on CuCeZr catalysts derived from UiO-66 metal organic frameworks, React. Kinet. Mech. Catal., 128 (2019) 193–204.
[4] X.D. Zhang, X.T. Lv, F.K. Bi, G. Lu, Y.X. Wang, Highly efficient Mn_2O_3 catalysts derived from Mn-MOFs for toluene oxidation: the influence of MOFs precursors, Mol. Catal., 482 (2019) 110701.
[5] X. Zou, C. Yuan, Y. Dong, H. Ge, J. Ke, Y. Cui, Lanthanum orthovanadate/bismuth oxybromide heterojunction for enhanced photocatalytic air purification and mechanism exploration, Chem. Eng. J., 379 (2020) 122380.
[6] C. Zhang, K. Zeng, C. Wang, X. Liu, G. Wu, Z. Wang, D. Wang, $LaMnO_3$ perovskites via a facile nickel substitution strategy for boosting propane combustion performance, Ceram. Int., 46 (2020) 6652–6662, doi: 10.1016/j.ceramint.2019.11.153.
[7] M. Zhou, Z. Wang, Q. Sun, J. Wang, C. Zhang, D. Chen, X. Li, High performance Ag-Cu nanoalloy catalyst for the selective catalytic oxidation of ammonia, ACS Appl. Mater. Interfaces, 11 (2019) 46875–46885, doi: 10.1021/acsami.9b16349.
[8] C. Zhou, N. Gao, Y. Deng, W. Chu, W. Rong, S. Zhou, Factors affecting ultraviolet irradiation/hydrogen peroxide (UV/H_2O_2) degradation of mixed N-nitrosamines in water, J. Hazard. Mater., 231–232 (2012) 43–48.
[9] W.H. Chu, N.Y. Gao, Y. Deng, B.Z. Dong, Formation of chloroform during chlorination of alanine in drinking water, Chemosphere, 77 (2009) 1346–1351.
[10] W.H. Chu, N.Y. Gao, Y. Deng, S.W. Krasner, Precursors of dichloroacetamide, an emerging nitrogenous DBP formed during chlorination or chloramination, Environ. Sci. Technol., 44 (2010) 3908–3912.
[11] W.H. Chu, N.Y. Gao, Y. Deng, M.R. Templeton, D.Q. Yin, Impacts of drinking water pretreatments on the formation of nitrogenous disinfection by-products, Bioresour. Technol., 102 (2011) 11161–11166.
[12] W.H. Chu, N.Y. Gao, Y. Deng, M.R. Templeton, D.Q. Yin, Formation of nitrogenous disinfection by-products from pre-chloramination, Chemosphere, 85 (2011) 1187–1191.
[13] W.H. Chu, N.Y. Gao, D.Q. Yin, Y. Deng, M.R. Templeton, Ozone-biological activated carbon integrated treatment for removal of precursors of halogenated nitrogenous disinfection by-products, Chemosphere, 86 (2012) 1087–1091.
[14] I.K. O'Neill, R.C.V. Borstel, C.T. Miller, J. Long, H. Bartsch, N-Nitroso Compounds: Occurrence, Biological Effects and Relevance to Human Cancer, IARC Scientific Publication No. 57, Oxford University Press, Lyon, 1984.
[15] W.F. Wang, S.Y. Ren, H.F. Zhang, J.W. Yu, W. An, J.Y. Hu, M. Yang, Occurrence of nine nitrosamines and secondary amines in source water and drinking water: potential of secondary amines as nitrosamine precursors, Water Res., 45 (2011) 4930–4938.
[16] T. Bond, J. Huang, M.R. Templeton, N. Graham, Occurrence and control of nitrogenous disinfection by-products in drinking water - a review, Water Res., 45 (2011) 4341–4354.
[17] J.M. Boyd, S.E. Hrudey, S.D. Richardson, X.F. Li, Solid-phase extraction and high-performance liquid chromatography mass spectrometry analysis of nitrosamines in treated drinking water and wastewater, TrAC Trends Anal. Chem., 30 (2011) 1410–1421.
[18] M.R. Templeton, Z. Chen, NDMA and seven other nitrosamines in selected UK drinking water supply systems, J. Water Supply Res.Technol. Aqua, 59 (2010) 277–283.
[19] California Department of Public Health, Notification Levels Overview, United States, 2006.
[20] California Department of Public Health, NDMA and Other Nitrosamines, Drinking Water Issues, United States, 2009.
[21] U.S. Environmental Protection Agency, Unregulated Contaminant Monitoring Rule 2 (UCMR2), United States, 2006.
[22] U.S. Environmental Protection Agency, United States Contaminant Candidate Llist 3-Final, 2009.
[23] C. Planas, O. Palacios, F. Ventura, J. Rivera, J. Caixach, Analysis of nitrosamines in water by automated SPE and isotope dilution GC/HRMS - occurrence in the different steps of a drinking water treatment plant, and in chlorinated samples from a reservoir and a sewage treatment plant effluent, Talanta, 76 (2008) 906–913.
[24] E. Bayram, N. Hoda, E. Ayranci, Adsorption/electrosorption of catechol and resorcinol onto high area activated carbon cloth, J. Hazard. Mater., 168 (2009) 1459–1466.
[25] M.I. Stefan, J.R. Bolton, UV direct photolysis of N-nitrosodimethylamine (NDMA): kinetic and product study, Helv. Chim. Acta, 85 (2002) 1416–1426.
[26] S. Liang, J.H. Min, M.K. Davis, J.F. Green, D.S. Remer, Use of pulsed-UV processes to destroy NDMA, J. Am. Water Works Assoc., 95 (2003) 121–131.
[27] W.A. Mitch, J.O. Sharp, R.R. Trussell, R.L. Valentine, L. Alvarez-Cohen, D.L. Sedlak, N-nitrosodimethylamine (NDMA) as a drinking water contaminant: a review, Environ. Eng. Sci., 20 (2003) 389–404.
[28] B. Ozkaya, Adsorption and desorption of phenol on activated carbon and a comparison of isotherm models, J. Hazard. Mater., 129 (2006) 158–163.
[29] S. Yenisoy-Karakas, A. Aygun, M. Gunes, E. Tahtasakal, Physical and chemical characteristics of polymer-based spherical activated carbon and its ability to adsorb organics, Carbon, 42 (2004) 477–484.
[30] C.M. Sharpless, K.G. Linden, Experimental and model comparisons of low- and medium-pressure Hg lamps for the direct and H_2O_2 assisted UV photodegradation of N-nitrosodimethylamine in simulated drinking water, Environ. Sci. Technol., 37 (2003) 1933–1940.
[31] M.H. Plumlee, M. Lopez-Mesas, A. Heidlberger, K.P. Ishida, M. Reinhard, N-nitrosodimethylamine (NDMA) removal by reverse osmosis and UV treatment and analysis via LC-MS/MS, Water Res., 42 (2008) 347–355.

[32] R.K. Singh, S. Kumar, S. Kumar, A. Kumar, Development of parthenium based activated carbon and its utilization for adsorptive removal of p-cresol from aqueous solution, J. Hazard. Mater., 155 (2008) 523–535.
[33] S.H. Lin, R.S. Juang, Adsorption of phenol and its derivatives from water using synthetic resins and low-cost natural adsorbents: a review, J. Environ. Manage., 90 (2009) 1336–1349.
[34] A. Kumar, S. Kumar, S. Kumar, Adsorption of resorcinol and catechol on granular activated carbon: equilibrium and kinetics, Carbon, 41 (2003) 3015–3025.
[35] K.P. Singh, A. Malik, S. Sinha, P. Ojha, Liquid-phase adsorption of phenols using activated carbons derived from agricultural waste material, J. Hazard. Mater., 150 (2008) 626–641.
[36] J. Deng, Y.S. Shao, N.Y. Gao, S.Q. Zhou, X.H. Hu, Adsorption characteristics of ss-Ionone in water on granular activated carbon, Clean – Soil Air Water, 40 (2012) 1341–1348.
[37] T. Calvete, E.C. Lima, N.F. Cardoso, S.L.P. Dias, E.S. Ribeiro, Removal of brilliant green dye from aqueous solutions using home made activated carbons, Clean – Soil Air Water, 38 (2010) 521–532.
[38] K.A. Krishnan, K.G. Sreejalekshmi, S. Varghese, T.S. Anirudhan, Removal of EDTA from aqueous solutions using activated carbon prepared from rubber wood sawdust: kinetic and equilibrium modeling, Clean – Soil Air Water 38 (2010) 361–369.
[39] X. Dai, L. Zou, Z. Yan, M. Millikan, Adsorption characteristics of N-nitrosodimethylamine from aqueous solution on surface-modified activated carbons, J. Hazard. Mater., 168 (2009) 51–56.
[40] H.J. Kim, H. Moon, H.C. Park, Multicomponent adsorption equilibria of phenols on activated carbon, Korean J. Chem. Eng., 2 (1985) 181–187.
[41] S.K. Srivastava, R. Tyagi, Competitive adsorption of substituted phenols by activated carbon developed from the fertilizer waste slurry, Water Res., 29 (1995) 483–488.
[42] S. Nouri, F. Haghseresht, G.Q.M. Lu, Comparison of adsorption capacity of p-Cresol & p-Nitrophenol by activated carbon in single and double solute, Adsorption, 8 (2002) 215–223.
[43] A. Leitao, R. Serrao, Adsorption of phenolic compounds from water on activated carbon: prediction of multicomponent equilibrium isotherms using single-component data, Adsorption, 11 (2005) 167–179.
[44] N. An, H.H. Xie, N.Y. Gao, Y. Deng, W.H. Chu, J. Jiang, Adsorption of two taste and odor compounds IPMP and IBMP by granular activated carbon in water, Clean – Soil Air Water, 40 (2012) 1349–1356.
[45] J. Chen, L. Gao, C. Shi, Y. Wang, D. Qi, Y. Hong, W. Shen, Y. Wang, J. Zhu, New versatile zincic sorbent for tobacco specific nitrosamines and lead ion capture, J. Hazard. Mater., 383 (2020) 121188.
[46] Y. Yang, J. Feng, S. Zhu, J. Zhou, K. Zhang, X. Ma, D. Gallagher, A.M. Dietrich, Activated carbon adsorption for removal of the nitrogenous disinfection byproduct phenylacetonitrile from drinking water, Desal. Water Treat., 166 (2019) 202–210.
[47] S. Li, C. Shi, Y. Wang, X. Sun, D. Qi, D. Wu, Y. Wang, J. Zhu, New efficient selective adsorbent of tobacco specific nitrosamines derived from discarded cigarette filters, Microporous Mesoporous Mater., 284 (2019) 393–402.
[48] C. Lin, C. Li, C. Chen, W. Chen, Removal of chlorpheniramine and variations of nitrosamine formation potentials in municipal wastewaters by adsorption onto the GO-Fe_3O_4, Environ. Sci. Pollut. Res. Int., 26 (2019) 20701–20711.
[49] R. Shen, S.A. Andrews, Demonstration of 20 pharmaceuticals and personal care products (PPCPs) as nitrosamine precursors during chloramine disinfection, Water Res., 45 (2011) 944–952.
[50] K.-j. Zhang, N.-y. Gao, Y. Deng, M.-h. Shui, Y.-l. Tang, Granular activated carbon (GAC) adsorption of two algal odorants, dimethyl trisulfide and β-cyclocitral, Desalination, 266 (2011) 231–237.
[51] Y.Y. Zhao, J. Boyd, S.E. Hrudey, X.F. Li, Characterization of new nitrosamines in drinking water using liquid chromatography tandem mass spectrometry, Environ. Sci. Technol., 40 (2006) 7636–7641.
[52] F. Inal, S. Yetgin, G.T. Aksu, S. Simsek, A. Sofuoglu, S.C. Sofuoglu, Activated carbon adsorption of fuel oxygenates MTBE and ETBE from water, Water Air Soil Pollut., 204 (2009) 155–163.
[53] R.S. Juang, F.C. Wu, R.L. Tseng, Mechanism of adsorption of dyes and phenols from water using activated carbons prepared from plum kernels, J. Colloid Interface Sci., 227 (2000) 437–444.
[54] F.Y. Wang, H. Wang, J.W. Ma, Adsorption of cadmium(II) ions from aqueous solution by a new low-cost adsorbent-Bamboo charcoal, J. Hazard. Mater., 177 (2010) 300–306.
[55] R.R. Sheha, E. Metwally, Equilibrium isotherm modeling of cesium adsorption onto magnetic materials, J. Hazard. Mater., 143 (2007) 354–361.
[56] D.H. Lataye, I.M. Mishra, I.D. Mall, Adsorption of alpha-picoline onto rice husk ash and granular activated carbon from aqueous solution: equilibrium and thermodynamic study, Chem. Eng. J., 147 (2009) 139–149.
[57] C. Pelekani, V.L. Snoeyink, Competitive adsorption in natural water: role of activated carbon pore size, Water Res., 33 (1999) 1209–1219.
[58] A.D. Mcnaught, A. Wilkinson, Compendium of Chemical Terminology: IUPAC Recommendations, Blackwell Science, Malden, MA, 1997.
[59] E. Tutem, R. Apak, C.F. Unal, Adsorptive removal of chlorophenols from water by bituminous shale, Water Res., 32 (1998) 2315–2324.

Supplementary information

Table S1
Molecular structures and physico-chemical parameters of NDPA and NDBA

Nitrosamines	Abbreviation	Molecular formula	Molecular weight (g/mol)	Structure	Boiling point (°C)	Solubility (g)	Unit cancer risk (10^{-6})	log (K_{ow})
Nitrosodipropylamine	NDPA	$[CH_3(CH_2)_2]_2\ N_2O$	130	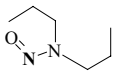	78	0.98	5 ng/L	1.36
Nitrosodibutylamine	NDBA	$[CH_3(CH_2)_3]_2\ N_2O$	144	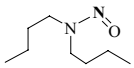	116	0.12	6 ng/L	2.63

Table S2
Physical and chemical properties of GAC

GAC	Particle size (mesh)	Apparent density (g/cm^3)	Intensity (%)	Dry weight (%)	Iodine (mg/g)	Methylene Blue value (mg/g)
MZ	8 × 30	476	93	10	950	180
YK	8 × 30	430–530	90	10	1,250	200
GK	8 × 30	350–430	90	10	1,080	200

Table S3
Structural characteristics of YK

Specific surface area (m^2/g)			Pore volume (cm^3/g)			Pore size (nm)	
BET	Micro[a]	BJH[b]	Total[c]	Micro[a]	BJH[b]	Average[d]	BJH[b]
925	912	299	0.457	0.433	0.177	1.97	2.36

[a]Micro: *t*-plot micropore.
[b]BJH: cumulative pores between 1.7 and 300 nm from BJH adsorption branch.
[c]Single point adsorption total pore volume at $P/P_0 > 0.99$ (corresponding to less than 200 nm pores).
[d]Adsorption average pore width (4 V/A by BET).

Table S4
Product ions, tube lens, and collision energies of NAms

NAms	Parent ion	Product ions	SRM collision energies	Tube lens
NDPA	131.310	43.6, 41.6, 39.6	14, 18, 34	75
NDBA	159.310	57.5, 41.6, 39.6	12, 18, 38	77

Table S5
Basic physical and chemical characteristics of the tap water and raw water

	Temperature (°C)	pH	Turbidity (NTU)	DOC (mg/L)	UV254	Hardness (mg/L)
Tap water	14.50	7.42	0.15	3.10	0.05	96.60
Raw water	7.50	8.02	3.00	5.31	0.12	199.00

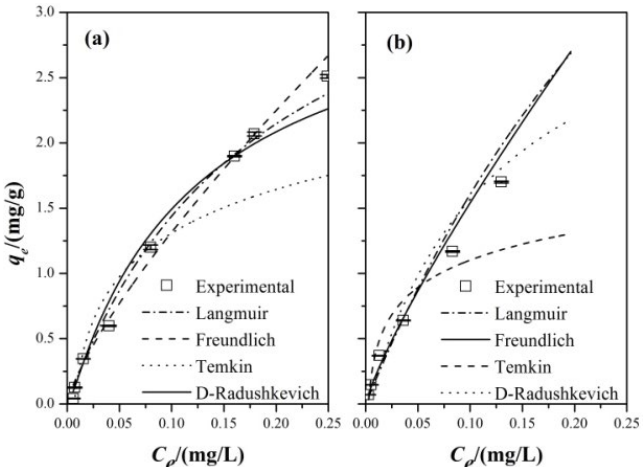

Fig. S1. Adsorption isotherms of GAC adsorption for a mixed solution of NDPA and NDBA at 288 K (initial concentrations = 0.01–0.50 mg/L, C_{YK} = 0.1 g/L, T = 288 K, pH = 7, t = 48 h) (a) NDPA and (b) NDBA.

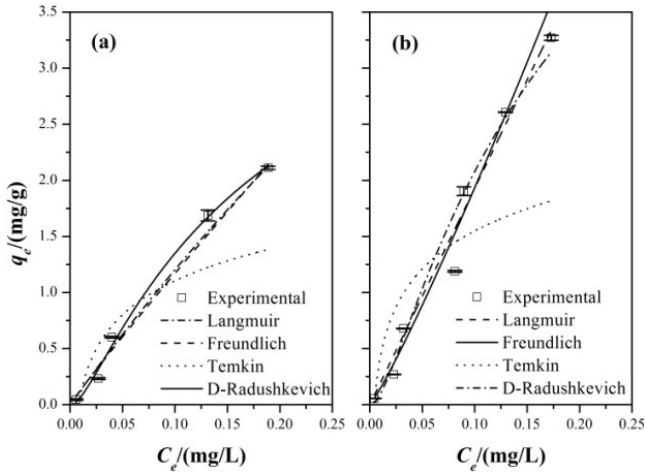

Fig. S2. Adsorption isotherms of GAC adsorption for a mixed solution of NDPA and NDBA at 298 K (initial concentrations = 0.01–0.50 mg/L, C_{YK} = 0.1 g/L, T = 298 K, pH = 7, t = 48 h) (a) NDPA and (b) NDBA.

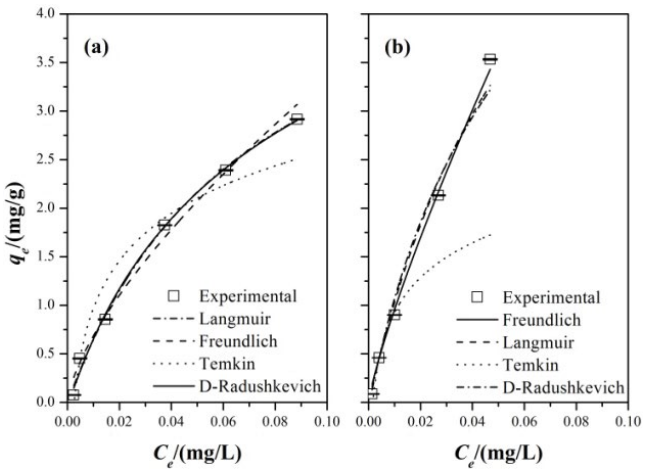

Fig. S3. Adsorption isotherms of GAC adsorption for a mixed solution of NDPA and NDBA at 308 K (initial concentrations = 0.01–0.50 mg/L, C_{YK} = 0.1 g/L, T = 308 K, pH = 7, t = 48 h) (a) NDPA and (b) NDBA.

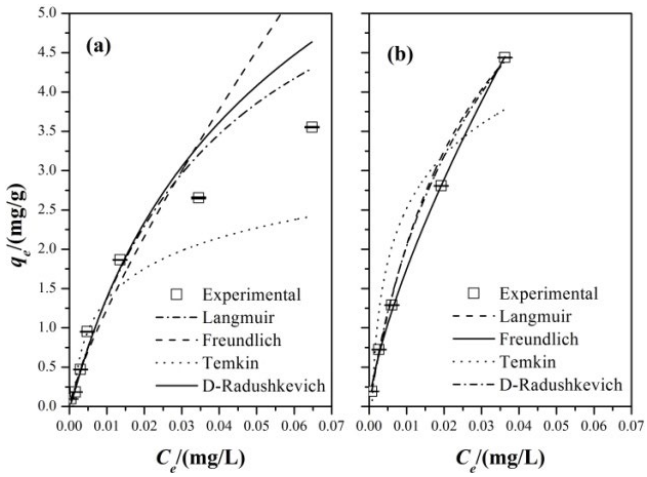

Fig. S4. Adsorption isotherms of GAC adsorption of a mixed solution of NDPA and NDBA at 318 K (initial concentrations = 0.01–0.50 mg/L, C_{YK} = 0.1 g/L, T = 318 K, pH = 7, t = 48 h) (a) NDPA and (b) NDBA.